Soft Matter

Accepted Manuscript

ROYAL SOCIETY OF CHEMISTRY

www.rsc.org/softmatter

Can the Scaling Behavior of Electric Conductivity be Used to Probe the Self-Organizational Changes in Solution with the Respect to the Ionic Liquid Structure? The case of $[C_8MIM][NTf_2]$

Marian Paluch[1,2*], Zaneta Wojnarowska[1,2], Peter Goodrich[3], Johan Jacquemin[3], Jürgen Pionteck[4] and Stella Hensel-Bielowka[5]

[1]*Institute of Physics, University of Silesia, Uniwersytecka 4, 40-007 Katowice, Poland.*
[2]*Silesian Center for Education and Interdisciplinary Research, 75 Pulku Piechoty 1A, 41-500 Chorzow, Poland.*
[3]*The School of Chemistry and Chemical Engineering/QUILL Research Centre, Queen's University of Belfast, David Keir Building, Stranmillis Road, Belfast BT9 5AG, Northern Ireland, UK.*
[4]*Leibniz Institute of Polymer Research Dresden, Hohe Str. 6, D-01069 Dresden, Germany.*
[5]*Institute of Chemistry, University of Silesia, Szkolna 9,40-006 Katowice, Poland.*

* Author to whom correspondence should be addressed: marian.paluch@us.edu.pl

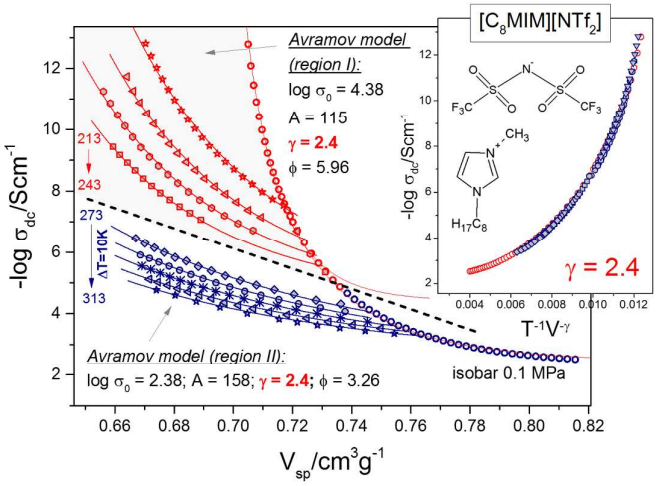

Scaling exponent as a key parameter to probe self-organization changes in solution with the respect to the IL structure

ABSTRACT: Electrical conductivity of the supercooled ionic liquid $[C_8MIM][NTf_2]$, determined as the function of the temperature and pressure, highlights strong differences in its ionic transport behavior between low and high temperature regions. To date, the crossover effect which is very well-known for low molecular van der Waals liquids is rarely described for classical ionic liquids. This finding highlights that the thermal fluctuations could be a dominant mechanism driving the dramatic slowing down of ion motions near T_g. An alternative way to analyze separately low and high temperature dc-conductivity data using a density scaling approach was then proposed. Based on which a common value of the scaling exponent γ=2.4 was obtained, indicating that the applied density scaling is insensitive to the crossover effect. By comparing scaling exponent γ reported herein along with literature data for other ionic liquids, it appears that γ decreases by increasing the alkyl chain length on the 1-alkyl-3-methylimidazolium-based ionic liquids. This observation may be related to changes in the interaction between ions in solution driven by an increasing of the van der Waals type interaction by increasing the alkyl chain length on the cation. This effect may be related to changes on the ionic liquid nanostructural organization with the alkyl chain length on the cation as previously reported in the literature based on molecular dynamic simulations. In other words, the calculated scaling exponent γ may be then used as a key parameter to probe the interaction and/or self-organizational changes in solution with the respect to the ionic liquid structure.

Keywords: Electric Conductivity, Ionic Liquids, High Pressure, Density Scaling

Introduction

The last decade has brought an impressive number of the works devoted to ionic liquids (ILs). To a large degree this is dictated by the fact that they are at the center of interest in both fundamental and applied research. The range of their industrial applications is diverse. For example, ILs are used in the chemical industry,[1] electrochemistry,[2] pharmacy,[3,4] catalysis,[5] *etc.* From the perspective of their applications in electrochemical devices,[6] a physical quantity of particular interest is an ionic dc-conductivity (σ_{dc}), and its dependence on temperature has also a practical meaning.

It is very well known that some ILs can be very easily supercooled below their melting point and by further cooling transformed into the disordered solids (glasses).[7] In this case, the dc-ionic conductivity will usually change by more than 12 decades achieving values of approximately 10^{-15} [$\Omega^{-1}\cdot cm^{-1}$] in the vicinity of the glass transition temperature (T_g). Since, in general, the ionic conductivity depends on the concentration of charge carriers and their mobility this enormous decrease in σ_{dc} value observed upon approaching T_g is mainly due to the dramatic slowing down of ionic movement. In the case of a simple thermally activated process, where an ion hopes over an energy barrier, the temperature dependence on σ_{dc} should follow the Arrhenius law (eq.1):

$$\sigma_{dc}(T) = \sigma_0 \exp(E_A/RT) \quad (1)$$

where σ_0 is a pre-exponential factor, E_A is the activation energy, and R is the universal gas constant.

However, it has been experimentally recognized that the $\sigma_{dc}(T)$ dependence is usually stronger than the simple Arrhenius behavior and for that reason it is often known as the super-Arrhenius behavior. This almost universal behavior can be rationalized on the basis of the cooperative nature of the ions' diffusion. It is nearly always reported that the three-parameter Vogel-Fulcher-Tammann (VFT) type fitting equation fairly well accounts the experimental data for σ_{dc} (eq.2):

$$\log_{10}\sigma_{dc}(T) = \log_{10}\sigma_0 + \frac{D_T T_0}{T - T_0} \quad (2)$$

where $\log_{10}\sigma_0$ is a pre-exponential factor, D_T is a material constant and T_0 is the temperature usually regarded as the 'ideal' glass temperature.

Naturally, the degree of deviation from the Arrhenius law is not the same for each IL and is determined by a number of factors like hydrogen bonding, van der Waals and Columbic forces along with the molecular volume of ions. From the thermodynamic point of view, the main factors controlling the conduction process are the thermal and density fluctuations. In general, both of them need to be taken into account when discussing the super Arrhenius behavior of the ionic conductivity. However, the relative importance of these factors on the conduction process is not yet clarified. In other words, to what extent is the deviation from the Arrhenius behavior a consequence of the variation in molecular packing upon approaching T_g. The only way to answer this question is through the use of pressure that allows the separation of the joint effects of temperature and molecular packing.[8] However, high pressure ionic conductivity measurements might pose a challenge for researchers due to some experimental difficulties to determine accurately this property. That is why little work in comparison to ambient pressure measurements has been done so far towards studying the effect of pressure on the ion conducting process in the vicinity of the glass transition.[9,10]

The main motivation of this letter was to establish whether molecular packing is a relevant parameter required to explain the evolution of dc-conductivity as the liquid-glass transition is approached. To address this problem, we carried out broadband dielectric studies of the IL 1-octyl-3-methylimidazolium bis[(trifluoromethyl)sulfonyl]imide [C_8MIM][NTf_2], which is one of the most typical ILs studied to date. The dielectric experiments were performed under both isothermal and isobaric conditions. However most of them were done isothermally. In addition, we also carried out pressure-volume-temperature (*PVT*), measurements. Thus, we were able to analyze thoroughly the charge transport in [C_8MIM][NTf_2] as a functions temperature, pressure and volume.

Experimental

Examined material

The sample under tests is ionic liquid 1-octyl-3-methylimidazolium bis[(trifluoromethyl)sulfonyl]imide [C_8MIM][NTf_2]. This sample was synthesized and purified in-house in the QUILL center within a purity, expressed in mole fraction unit, close to 99%. Details about sample preparation and purification are presented in electronic supporting information.

Dielectric measurements

Ambient pressure dielectric measurements of $[C_8MIM][NTf_2]$ were performed over a wide frequency range from 10^{-1} to 10^6 Hz using a Novo-Control GMBH Alpha dielectric spectrometer. During the ambient pressure measurements the sample was placed between two round stainless steel electrodes of the capacitor (diameter 10 mm). Silica spacers of 100 μm diameter were used to ensure constant sample thickness. The temperature was controlled by the Novo-Control Quattro system, with the use of a nitrogen gas cryostat. Temperature stability of the samples was better than 0.1 K.

For the pressure dependent BDS experiment the stainless steel capacitor (square-shape electrodes with plate's area the same as for ambient pressure measurements, separated with silica spacers 100 μm) was used. It was next installed in a special holder, covered by a Teflon capsule and filled with a tested liquid. Such a prepared sealed cell was next placed in the high-pressure chamber and compressed by means of a hydraulic pump using a nonpolar pressure-transmitting liquid (silicon oil). Note, the examined sample was in contact only with stainless steel and Teflon. The general scheme of the apparatus used to investigate the properties of $[C_8MIM][NTf_2]$ under high pressure conditions is presented in ref [11]. The pressure was measured by using a Nova Swiss tensometric pressure meter with a resolution of 0.1 MPa. The temperature was controlled within 0.1 K by means of Weiss fridge. The ambient and high pressure dielectric measurements were performed within the linear response regime, with voltage of 1 V. Standard uncertainty is $\log_{10}\sigma_{dc} = 0.001$ S/cm.

Pressure-volume-temperature (PVT) measurements

The PVT experiments of the $[C_8MIM][NTf_2]$ were carried out using a fully automated GNOMIX high pressure dilatometer[12,13]. The apparatus is described elsewhere.[14] The principle of the GNOMIX-PVT apparatus is the confining fluid technique. About 1.9 g of the IL has been added into the cell and the remaining cell volume was filled with mercury acting as a confining fluid, which ensures that the material is under hydrostatic pressure at all times. PVT data in the range from 20 MPa to 200 MPa in increments of 20 MPa, and from room temperature up to 393 K in steps of 5 K have been collected in the isothermal standard mode. The values for 0.1 MPa are obtained by extrapolation according to the Tait equation for each temperature using the standard PVT software. In the studied range the accuracy limit for the absolute values of the specific volume is within 0.002 cm^3/g.

Results and Discussion

The key quantity considered throughout this work is the ionic dc-conductivity determined from broadband dielectric spectroscopy (BDS) measurements. The obtained experimental data can be presented and analyzed in a variety of representations, *i.e.:* the complex dielectric permittivity $\varepsilon^*(\omega) = \varepsilon'(\omega) - i\varepsilon''(\omega)$, complex electric modulus $M^*(\omega) = M'(\omega) + iM''(\omega)$ and complex electric conductivity $\sigma^*(\omega) = \sigma'(\omega) + i\sigma''(\omega)$. However, all these quantities are interrelated to each other: $\varepsilon^*(\omega) = 1/M^*(\omega) = \sigma^*(\omega)/i\omega\varepsilon_0$ and therefore contain the same information about the processes of relaxation and conduction in materials.[15] These various formalisms are used just to emphasize the different aspects of the same phenomenon. In the case of conducting materials the $\sigma^*(\omega)$ representation is preferred because the dc conductivity can be easily identified and determined as will be discussed later. A few exemplary spectra of electrical conductivity obtained at various temperature conditions and ambient pressure for $[C_8MIM][NTf_2]$ are displayed in 3D plot in Figure 1a. Aside from the ambient pressure studies we also carried out a number of isothermal measurements as a function of compression (see Figure 1b). In the presented spectra three characteristic dispersive regions can be identified. Starting from the highest to the lowest frequencies, one can observe that the electric conductivity sharply decreases according to a power law and reaches the plateau value. This constant value determines the dc-conductivity which varies both with temperature and pressure. It is obvious from Figures 1a and 1b that cooling and compression basically exert the same effect on the behavior of σ_{dc}. As the movement of the ions is limited by the surface of the capacitor plates it results in the gradual dropping of the conductivity at the lower frequencies. This phenomenon is well known as an electrode-blocking effect.

As outlined above, the values of σ_{dc} at various T and P conditions were determined directly from the plateau region on the conductivity spectra. The isobaric and isothermal dependences on σ_{dc} are shown separately in Figures 2a and 2b, respectively. The isobaric data are plotted versus inverse of temperature to emphasize their super-Arrhenius behavior. In such cases, the experimental data are often well described by the three-parameter type fitting VFT equation (eq.2). However, as we found from the fitting analysis, this procedure is not valid for $[C_8MIM][NTf_2]$. As shown in Figure 2a, two VFT laws are required to parameterize the data over the entire temperature range. This fact suggests the occurrence of high temperature "crossover" effect that is rarely observed in the case of ILs. It might be due to the fact that ILs in general, exhibit much weaker crossover effects when compared to low molecular van der

Waals liquids. Differences in ionic transport behavior between low and high temperature regions are also manifested in Figure 2b. As shown in this figure, isotherms measured at higher temperatures exhibit a linear dependence which agrees well with the prediction of simple volume activated model (eq.3).

$$\log_{10}\sigma_{dc}(P) = \log_{10}\sigma_0 + \frac{P\Delta V}{RT} \tag{3}$$

where ΔV is an activation volume and $\log_{10}\sigma_0$ is the value of dc conductivity at atmospheric pressure.

On the other hand, the above equation fails to describe low temperature isotherms due to their strongly non-linear character indicating the absence of a single activated volume over the entire pressure range. This feature can be captured by using the pressure counterpart of the temperature VFT law (eq.4).[16]

$$\log_{10}\sigma_{dc}(T) = \log_{10}\sigma_0 + \frac{D_P P}{P_0 - P} \tag{4}$$

The effectiveness of the eq.4 for the description of low temperature isotherms is demonstrated as exemplified in Figure 2b. From above discussion, it is concluded that the crossover effects can also be revealed when we analyze both high and low temperature isotherms.

In order to determine the contributions of both density and thermal fluctuations in the super Arrhenius behavior of $\sigma_{dc}(T)$ dependence, data under isochoric conditions are also required. For this purpose, we additionally performed *PVT* measurements which are presented in Figure 2c. The temperature range covered in this study was from (297 to 395) K and differs somewhat from that covered in the dielectric measurements. Therefore, the collected *PVT* data were then parameterized by means of an equation of state (eq.5),[17,18] and extrapolated to lower temperatures based on the values of parameters obtained from the fitting procedure.

$$\left(\frac{v(T,p_0)}{v(T,p)}\right)^{\gamma_{EOS}} = 1 + \frac{\gamma_{EOS}}{B_T(p_0)}(p - p_0) \tag{5}$$

where: $B_T(p_0) = B_{T_0}(p_0)\exp(-b_2(T - T_0))$ and $v(T,p_0) = A_0 + A_1(T - T_0) + A_2(T - T_0)^2$

Having the parameterized *PVT* data, it is now possible to plot the temperature dependence of σ_{dc} at constant volume (see Figure 3). From the Figure 3, it is evident that the isochoric curves also exhibit super-Arrhenius behavior. For comparison, we included also in Figure 3 the isobaric dependence on σ_{dc}. A relative importance of the thermal and density fluctuation can be assessed based on the value of the ratio of the apparent activation enthalpy at constant

volume to the activation enthalpy at constant pressure.[19] In practice, it requires the determination of both these parameters from analysis of isochoric and isobaric $\sigma_{dc}(T)$ dependences by using:

$$H_V = R\left.\frac{\partial \ln \sigma_{dc}}{\partial T^{-1}}\right|_V \quad (6)$$

$$H_P = R\left.\frac{\partial \ln \sigma_{dc}}{\partial T^{-1}}\right|_P \quad (7)$$

For purposes of the computation of H_V (eq.6) and H_P (eq.7), we used the parameters obtained from fitting the VFT equation to the experimental data shown in Figure 3 and tabulated in the electronic supporting information. The ratio H_V/H_P is plotted as a function of $-\log\sigma_{dc}(T)$ in the inset of Figure 3. The value is nearly constant and equal to 0.79±0.02 indicating that when approaching the glass transition at ambient pressure the temperature is the dominant control variable responsible for the dramatic slowing down of ion mobility. This finding is different from that reported for simple van der Waals liquids.[8] Usually, for this type of liquid, the value of the ratio lies in the range from 0.40 to 0.55 which means that the density and thermal energy have nearly the same effect. However, a weaker effect of the density is commonly observed in the case of associated liquids and is comparable to what we found herein for [C_8MIM][NTf_2]. A common feature of associated liquids with strong hydrogen-bonding interactions is the existence of hydrogen-bonded clusters or networks. Since, in the case of associated liquids the characteristic value of ratio H_V/H_P is usually close to unity,[8] thermal fluctuations become a main driving force for breaking H-bonding and facilitating the molecular rearrangements. The large value of ratio H_V/H_P obtained for [C_8MIM][NTf_2] could also be related to strong nanostructural organizations previously postulated based on the molecular dynamic simulations.[20] From the simulations of the imidazolium-based ILs with varying the alkyl side-chain length ([C_nMIM][PF_6], with n = 2, 4, 6, 8 or 12) it was observed that polar and nonpolar domains are already formed for n = 4 and the non-polar domains become larger and more connected as the length of the alkyl chain increases. Thus, there is a straightforward analogy to associated liquids which explains why temperature is the dominant control variable in the case of [C_8MIM][NTf_2]. Finally, it is also interesting to determine the effect of compression on the ratio of H_V/H_P. By performing the analysis similar to that presented above, we see that the ratio increases with pressure (see lower inset in Figure 3). Thus, it can be concluded that compression enhances the role of thermal fluctuations.

An alternative approach to analysis of thermal and density effects is in terms of the density scaling.[21] This approach entails using a new variable: TV^{γ} which was previously

demonstrated to lead to the superposition of high pressure viscosity data (or the structural relaxation times) into a single master curve. The validity of the density scaling was proved experimentally for van der Waals liquids, polymers and more recently also for some ILs.[22] The scaling exponent γ reflects the relative contributions of thermal and density effects on the ion transport and for that reason it can be considered as an alternative measure of these effects. In the limiting cases, when γ tends to zero or infinity then thermal activation or free volume, respectively, become dominant. In this context, it is worth noting that the scaling exponent γ is related to the ratio H_V/H_P by[23]

$$\left.\frac{H_V}{H_p}\right|_{T=T_g} = \frac{1}{1+\gamma T_g \alpha_p(T_g)} \tag{8}$$

The other interesting point is that the scaling exponent γ is believed to be also related to the steepness of the repulsive intermolecular potential in solution. In fact, based on the numerous molecule dynamics simulations of van der Waals liquids, it was pointed out that values of the scaling exponent γ and the exponent in the inverse power law describing the intermolecular repulsive potential are nearly the same.[24,25] Undoubtedly, this is a very appealing perspective as one can get insight into the microscopic interactions between molecules in solution from the macroscopic measurements. Thus, we will further focus on the application of the density scaling idea to analysis the conductivity data of $[C_8MIM][NTf_2]$. As a starting point, we recalled the entropic Avramov model[26] used by Casalini, Mohanty and Roland[27] to derive the equation which establishes the functional relationship between the viscosity, η, and TV^{γ} Avramov parameter (eq.9).

$$\log_{10}\eta(T,V) = \log_{10}\eta_0 + \left(\frac{A}{TV^{\gamma}}\right)^{\phi} \tag{9}$$

In fact, this is the first theoretical approach that confirms the density scaling concept. Here, eq.9 was used to analyze the dc conductivity data as shown in Figure 4. However, from the numerical fitting procedure we found that eq.9 cannot describe the experimental data over the whole range of σ_{dc}. If there is a lack of satisfactory fit at this step, it can be attributed to the existence of a crossover effect as already highlighted above. Therefore, we repeated this process by fitting the high and low conductivity data separately. The dotted line in Figure 4 indicates a border between these two sets of the data, which corresponds to the high and low temperature regions. As can be seen very good fits with the resulting values of the fitting parameters presented in Figure 4, were obtained. The most interesting outcome of this analysis is that the same value of exponent γ was obtained for both sets of the data whereas

the other fitting parameters take different values. This means that the density scaling is insensitive to crossover effects, *i.e.* the same value of exponent γ describes high and low temperature regions. How it works in practice is illustrated in Figure 5. It is now evident that all isothermal and isobaric curves can be collapsed into a master curve using a common value of the scaling exponent γ=2.40±0.05. At this point, it is instructive to mention that the value of scaling exponent γ can be also determined from model independent analysis. At a given value of σ_{dc} the product $T_\sigma V_\sigma^\gamma = const$, which results directly from the density scaling law, leads to linear logarithmic dependence $T_\sigma(V_\sigma)$:

$$\log_{10} T_g = const - \gamma \log_{10} V_g \quad (10)$$

offering a simple method of determining the scaling exponent γ. From the linear regression (eq.10) to the data shown in the inset to Figure 5, we found γ = 2.4 which nicely agrees with the result from the previous analysis obtained using the Avramov model (eq.9).

For completeness of our discussion, we then recalled some experimental results obtained for other ILs. Very recently, our group reported that the γ value of $[C_4MIM][NTf_2]$ is equal to 3.0.[28] On first sight, it appears that the γ parameter seems to decrease with an increase in the alkyl chain length on the imidazolium cation. This decrease can be related to the well-known variation of volumetric properties as the function of the alkyl chain length on this cation.[29] Surprisingly, the same pattern emerges by solely taking into account transport properties results. For example, from high pressure viscosity studies of 1-alkyl-3-methylimidazolium hexafluorophosphate $[C_nMIM][PF_6]$ with n = 4 or 8 published by Roland *et al*.[30] γ values close to 2.9 and 2.4 were reported for $[C_4MIM][PF_6]$ and $[C_8MIM][PF_6]$, respectively. In other words, both the volumetric and transport properties analyses seem to lead to similar conclusions, which can be related to the specific interactions in these ILs. In fact, this structure-properties relationship should be considered in the light of the findings from MD simulations already mentioned above.[20] The observed decrease of the γ with an increase of the alkyl chain length on the imidazolium cation corresponds to the formation of larger and more connected nanostructures. This is a meaningful result because the scaling exponent γ may reflect the degree of self-organization evolving with the change of the alkyl side-chain length in some ILs.

Conclusions

To sum up, we have studied the isobaric and isothermal dependences on the ionic conductivity of $[C_8MIM][NTf_2]$ by means of broadband dielectric spectroscopy in broad

temperature and pressure ranges. The dc-conductivity data at atmospheric pressure reveal a high temperature crossover effect, which is also supported by isothermal data. A second important point is that the thermal fluctuations could be a dominant mechanism driving the dramatic slowing down of ion motions near T_g. We also presented an alternative way to analyze high-pressure dc-conductivity data based on a density scaling approach. In this connection, we then compared our results with other published data for different ILs and found that their structure affects strongly the scaling exponent γ of electric conductivity. This data analysis also highlights that this scaling exponent γ may be used as a key parameter to probe interaction and/or self-organization changes in solution with the respect to the IL structure.

AUTHOR INFORMATION

Notes

The authors declare no competing financial interest.

ACKNOWLEDGMENTS

The authors Z.W. and M.P. are deeply grateful for the financial support by the National Science Centre within the framework of the Opus project (Grant No. DEC 2011/03/B/ST3/0207.). Z.W. acknowledges financial assistance from FNP START 2014.

Supporting Information Available:

Experimental details, raw data collected during this work (Tables S1 and S2) and fitting parameters of pVFT equation and volume activated model (Table S3) can be found in the Electronic Supporting Information. This material is available free of charge via the Internet at http://pubs.acs.org.

Figures

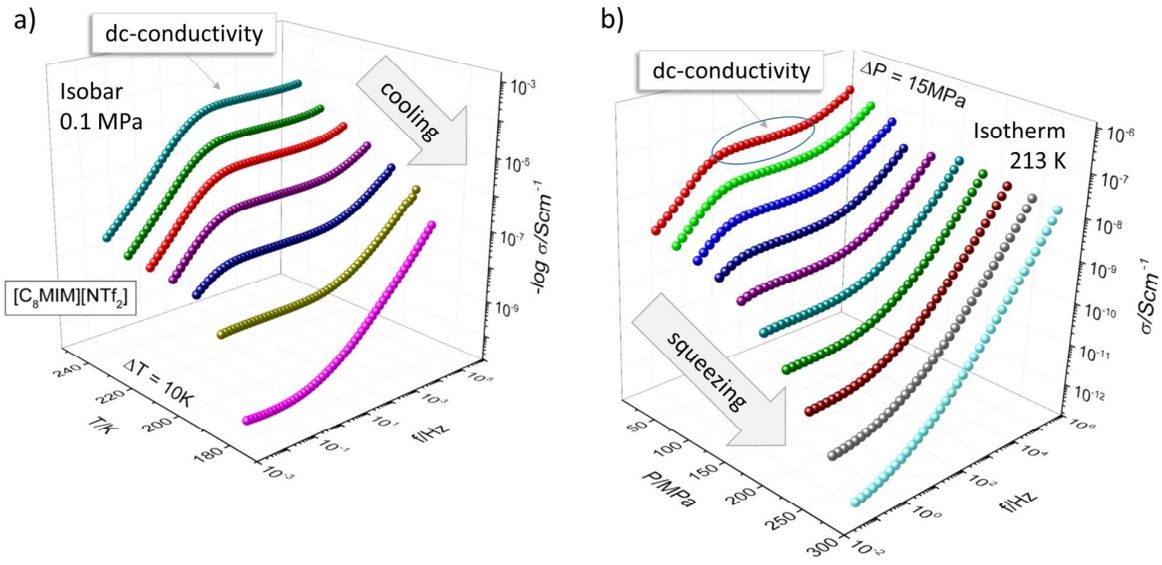

Figure 1. Dielectric relaxation spectra of $[C_8MIM][NTf_2]$ presented in the conductivity representation in the form of frequency dependent data measured at various (a) temperature and (b) pressure conditions.

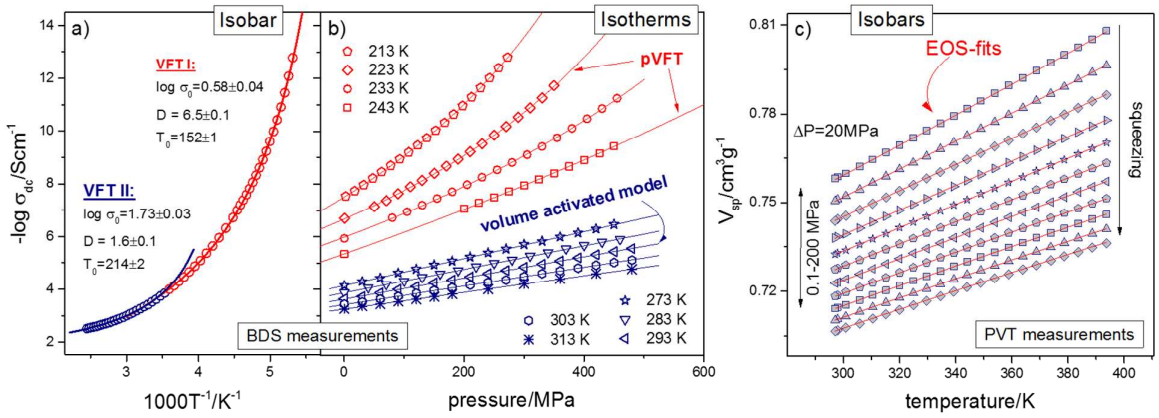

Figure 2. Panels (a) and (b) present the dc-conductivity data of $[C_8MIM][NTf_2]$ measured at various isobaric and isothermal conditions, respectively. Solid red lines are fits of pVFT equation to the experimental data with the parameters collected in supporting materials. Panel (c) presents the isobaric dependence of volume in the pressure range of 0.1–200 MPa. PVT data have been parameterized by means of equation of state with the following parameters: A_0= 0.704 cm^3/g, A_1=4.665·$10^{-4}$$cm^3/(g·K)$, A_2=1.59·10^{-7} $cm^3/(g·K^2)$, $B_T(P_0)$= 3139 MPa, b=0.00421 K^{-1}, γ_{EOS}=10.1, T_0= 185.96 K

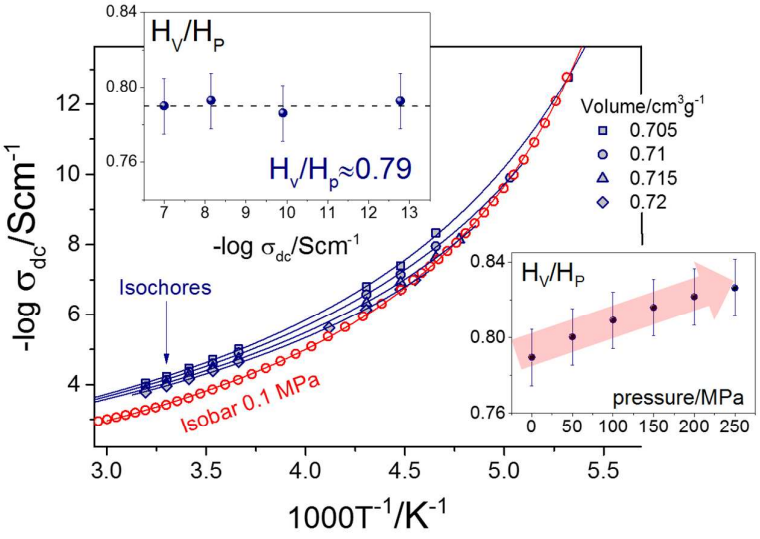

Figure 3. The temperature dependence on dc-conductivity at constant volume condition. The open circles represent the dependence on dc-conductivity at 0.1 MPa. The upper inset shows the ratio of the activation enthalpy at constant volume to the enthalpy change at constant pressure as a function of logσ_{dc}. On the other hand, the lower inset presents the pressure dependence of H_V/H_P ratio.

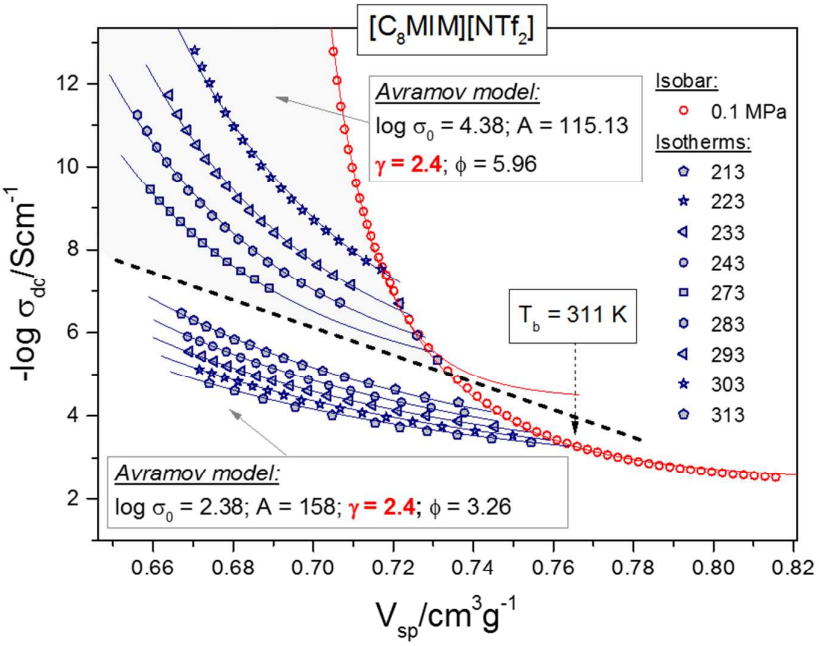

Figure 4. Isothermal and isobaric data for [C_8MIM][NTf_2] plotted as a function of volume. Solid lines are fits obtained using the eq.9.

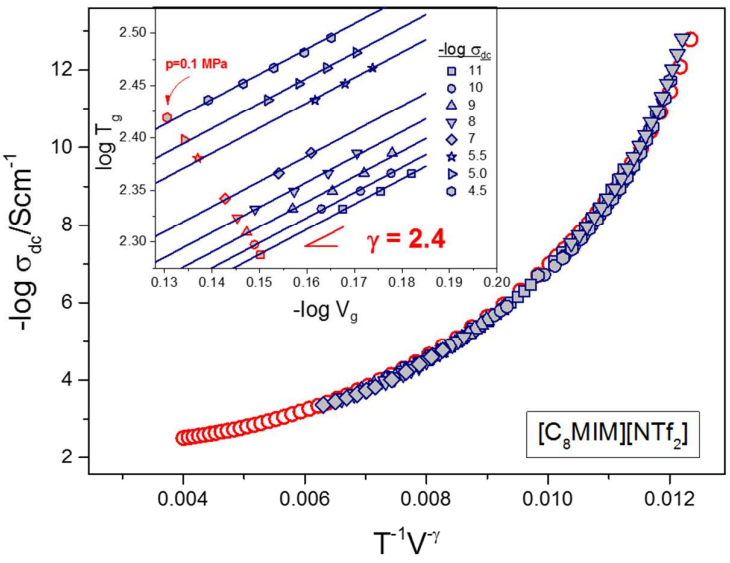

Figure 5. The electrical conductivity data for $[C_8MIM][NTf_2]$ plotted versus $(TV^{\gamma})^{-1}$ with the scaling exponent calculated herein as $\gamma = 2.4$. The inset shows the scaling exponent determined from the linear regression of the logarithmic dependence of glass transition temperature on volume. The solid lines denote the regression lines.

REFERENCES

(1) Plechkova, N. V.; Seddon, K. R. *Chem. Soc. Rev.* **2008**, *37*, 123-150.
(2) *Electrochemical Properties and Applications of Ionic Liquids,* Torriero, A. A. J.; Shiddiky, M. J. A., Eds. *Nova Science Publishers* **2011**.
(3) Wojnarowska, Z.; Paluch, M.; Grzybowski, A.; Adrjanowicz, K.; Grzybowska, K.; Kaminski, K.; Wlodarczyk, P.; Pionteck, J. *J. Chem. Phys*. **2009**, *131*, 104505.
(4) Wojnarowska, Z.; Grzybowska, K.; Hawelek, L.; Swiety-Pospiech, A.; Masiewicz, E.; Paluch, M.; Sawicki, W.; Chmielewska, A.; Bujak, P.; Markowski, J. *Mol. Pharmaceutics* **2012**, *9*, 1250-1261.
(5) Pârvulescu, V. I.; Hardacre, C. *Chem. Rev.* **2007**, *107*, 2615-2665.
(6) Armand, M.; Endres, F.; MacFarlane, D. R.; Ohno, H.; Scrosati, B. *Nat. Mater.* **2009**, *8*, 621-629.
(7) Sangoro, J. R.; Kremer, F. *Acc. Chem. Res.* **2012**, *45*, 525-532.
(8) Floudas, G.; Paluch, M.; Grzybowski, A.; Ngai, K.L. Molecular Dynamics of Glass-Forming Systems: Effects of Pressure. In: Kremer, F. (Ed.). *Advances in Dielectrics*. Berlin: Springer; **2011**.
(9) Paluch, M.; Haracz, S.; Grzybowski, A.; Mierzwa, M.; Pionteck, J.; Rivera-Calzada, A.; Leon, C. J. *Phys. Chem. Lett.* **2010**, *1*, 987-992.
(10) Harris, K. N.; Kanakubo, M*Faraday Discuss.* **2012**, *154*, 425-438.
(11) Wojnarowska, Z. Paluch, M. J. Phys.: Condens. Matter 27 (2015) 073202
(12) GNOMIX INC., 3809 Birchwood Drive, Boulder, CO 80304,USA.
(13) P. Zoller and D.Walsh, Standard Pressure–Volume–Temperature Data for Polymers, Technomic, Lancaster, PA, 1995.
(14) Y. A. Fakhreddin and P. Zoller, Society of Plastic Engineers ANTEC'91, 1991, vol. 36, p. 1642.
(15) Kremer, F.; Schoenhals, A. (Eds.). *Broadband Dielectric Spectroscopy.* Berlin: Springer; **2003**.
(16) Paluch, M.; Rzoska, S. J.; Habdas, P.; Ziolo, J. *J. Phys.: Condens. Matter* **1998**, *10*, 4131-4138.
(17) Grzybowski, A.; Paluch, M.; Grzybowska, K. *J. Phys. Chem. B* **2009**, *113*, 7419-7422.
(18) Grzybowski, A.; Koperwas, K.; Paluch, M. *J. Chem. Phys.* **2014**, *140*, 044502.
(19) Paluch, M.; Casalini, R.; Roland, C. M. *Phys. Rev. B* **2002**, *66*, 092202.
(20) Canongia Lopes, J. N. A.; Padua, A. A. H. *J. Phys. Chem. B* **2006**, 110, 3330-3335.
(21) Roland, C. M.; Hensel-Bielowka, S.; Paluch, M.; Casalini, R. *Rep. Prog. Phys.* **2005**, *68*, 1405-1478.
(22) M. Paluch, E. Masiewicz, A. Grzybowski, S. Pawlus, J. Pionteck and Z. Wojnarowska J. Chem. Phys. **2014**, 141 , 134507
(23) Casalini, R; Roland, C. M. *Phys. Rev. E* **2004**, *69*, 062501.
(24) Bailey, N. P.; Pedersen, U. R.; Gnan, N.; Schroder, T. B.; Dyre, J. C. *J. Chem. Phys.* **2008**, *129*, 184507.
(25) Coslovich, D.; Roland, C. M. *J. Chem. Phys*. **2009**, *130*, 014508.
(26) Avramov, I. *J. Non-Cryst. Solids* **2000**, *262*, 258-263.
(27) Casalini, R.; Mohanty, U.; Roland, C.M. *J. Chem. Phys.* **2006**, *125*, 014505.
(28) Wojnarowska, Z.; Jarosz, G.; Grzybowski, A.; Pionteck, J.; Jacquemin, J.; Paluch, M. *Phys. Chem. Chem. Phys*. **2014**, *16*, 20444-20450.
(29) Rooney, D.; Jacquemin, J.; Gardas, R. *Top. Curr. Chem.* **2009**, *290*, 185-212.
(30) Roland, C.M.; Bair, S.; Casalini, R. *J. Chem. Phys.* **2006**, *125*, 124508.

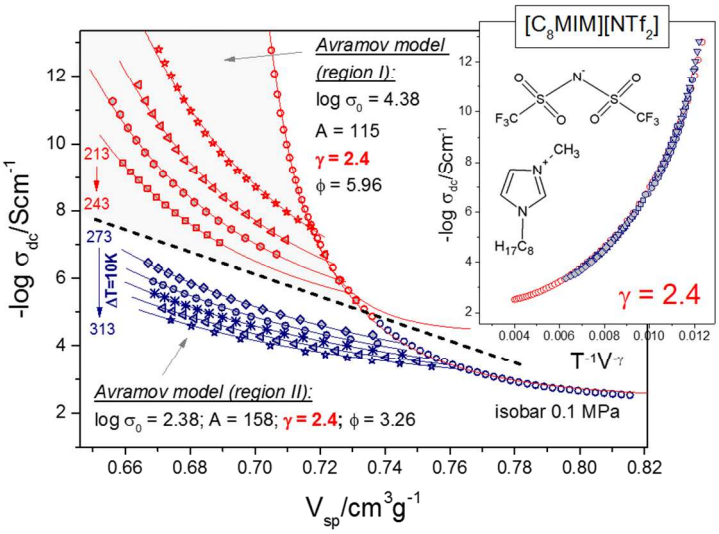

338x190mm (96 x 96 DPI)